Putting the silicon cycle in a bag: Field and mesocosm observations of silicon isotope fractionation in subtropical waters east of New Zealand

Meyerink, SW

1   **Putting the silicon cycle in a bag: Field observations of silicon isotope fractionation in**

2   **subtropical waters east of New Zealand**

3

4   Scott W. Meyerink[1#], Philip W. Boyd[2,3], William A. Maher[4], Angela Milne[5], Robert Strzepek[2,3]

5   and Michael J. Ellwood[1#]

6

7   1. Research School of Earth Sciences, Australian National University, Canberra,
8   Australia
9
10   2. Department of Chemistry, NIWA/University of Otago Research Centre for
11   Oceanography, University of Otago, Dunedin, New Zealand
12
13   3. Now at: Institute for Marine and Antarctic Studies and Antarctic Climate and
14   Ecosystems Co-operative Research Centre, University of Tasmania, Hobart,
15   Australia
16
17   4. Ecochemistry Laboratory, Institute for Applied Ecology, University of Canberra,
18   Bruce, Australia.
19
20   5. School of Geography, Earth and Environmental Sciences, University of Plymouth,
21   Plymouth PL4 8AA, United Kingdom
22
23   # corresponding authors: scott.meyerink@anu.edu.au; michael.ellwood@anu.edu.au

24

Abstract

A mesocosm experiment was used to investigate the fractionation of silicon (Si) isotopes in subtropical surface waters east of New Zealand. This region surface waters were characterised by relatively low concentrations of silicic acid ($Si(OH)_4$) (~2 µmol L^{-1}) and higher nitrate (~5 µmol L^{-1}) and dissolved iron (Fe) concentrations (~0.4 nmol L^{-1}) prior to development of the annual springtime phytoplankton bloom. To simulate initiation of the bloom, a large (~700 L) mesocosm experiment was undertaken whereby surface seawater containing the natural plankton community was incubated for a 168-hr period. During the mesocosm experiment the concentrations of $Si(OH)_4$, nitrate, phosphate and dissolved iron all decreased while the concentration of biogenic silica (BSi) increased 12-fold. Coupled with the increase in BSi was a change in the Si-isotope composition of BSi ($\delta^{30}Si_{BSi}$) which increased from 1.49 ‰ to 2.64 ‰ after 168 hr. Complementary observations to those made for the mesocosm experiment were made for corresponding surface waters. For these waters we observed a small decline in the concentrations of nitrate, phosphate and dissolved Fe, but little change in the concentrations of $Si(OH)_4$ and BSi. In contrast to the mesocosm experiment, surface water $\delta^{30}Si_{BSi}$ values became lighter during bloom initiation, suggestive of $Si(OH)_4$ being replenished into surface waters. These differences in the drawdown and utilisation of nutrients and dissolved Fe between the mesocosm and surface waters during bloom initiation likely result from favourable Fe and light supply conditions within the mesocosm. In contrast, water column stability (i.e. vertical mixing), and the supply of dissolved Fe are likely to influence bloom initiation and its longevity. The fractionation of Si-isotopes in the mesocosm experiment followed closed-system Rayleigh fractionation kinetics, and an enrichment factor (ε) of -1.13 ‰ was calculated for the exponential phase of growth for the diatom community, which was marked by the presence of the diatoms *Asterionelopsis glacilis* and *Mellosira moniliformis*. The isotope enrichment factor agreed well with previous observations of Si isotope fraction in diatoms from field communities, and appeared to be independent of variations in the ambient $Si(OH)_4$ concentration, and phytoplankton species composition.

1. Introduction

The biological fractionation of silicon (Si) isotopes by diatoms in the surface ocean makes the stable isotope composition of biogenic silica ($\delta^{30}Si_{BSi}$) an extremely sensitive tracer of the marine biogeochemical Si-cycle (de Souza et al., 2012b; Sutton et al., 2018). Understanding the processes governing Si-isotope fractionation is particularly important in the Southern Ocean, a region where silicic acid ($Si(OH)_4$) is retained as a result of diatoms in sub-polar waters preferentially removing $Si(OH)_4$ relative to nitrate (NO_3^-) from the water column. These Si-poor waters extend northward as Sub-Antarctic Mode Water (SAMW) and play a significant role in setting the nutrient status of the global ocean (Sarmiento et al., 2004). The strong de-coupling of $Si(OH)_4$ and NO_3^- in Antarctic polar waters has a particularly important bearing on marine productivity at lower latitudes, and is due to a complex interplay between, (1) different diatom species and morphological types displaying varying degrees of bio-silicification (Baines and Pace, 1991), (2) Fe and light limitation inducing heavier rates of bio-silicification and reduced uptake of NO_3^- in diatoms (Brzezinski et al., 2002; Franck et al., 2003; Marchetti et al., 2010), (3) the export and deep remineralisation of $Si(OH)_4$ relative to NO_3^- (Pichevin et al., 2014; Sarmiento et al., 2007), and (4) grazer induced variations in cell wall bio-silicification and cell morphology (Smetacek et al., 2004). Deciphering the relative importance of these processes is key to understanding the nutrient distribution in and outside of the Southern Ocean (Sarmiento et al., 2004).

The distribution of $\delta^{30}Si_{BSi}$ is extremely sensitive to these processes and acts as a useful tracer for examining the cycling of Si in resident diatom communities (De La Rocha et al., 1997; Fripiat et al., 2012; Milligan et al., 2004). The uptake of $Si(OH)_4$ by diatoms in the ocean influences the isotopic compositions of both $Si(OH)_4$ and biogenic silica (BSi) in surface waters. During $Si(OH)_4$ uptake, the lighter Si isotope (^{28}Si) is preferentially taken up, and is defined by a fractionation factor (ε). For laboratory cultures and field populations of diatoms ε generally ranges between -0.53 and -1.9 ‰, with the odd individual species having more extreme values e.g. *Chaetoceros brevis* (Cardinal et al., 2007; De La Rocha et al., 1997; Fripiat et al., 2011; Meyerink et al., 2017; Sutton et al., 2013; Varela et al., 2004). In general, the factors that influence Si silicon isotope fractionation during a phytoplankton bloom formation are not well characterised. The aim of this study was to simulate the formation of the annual spring bloom using mesocosm approach and complement mesocosm observations with water column measurements.

84   This study took place within a warm-core eddy (39°20S 180°00'W) east of New Zealand where

85   an annual spring phytoplankton bloom has been observed to occur based on satellite and field

86   measurements (Boyd et al., 2012; Ellwood et al., 2015; Murphy et al., 2001). The region is a

87   site of considerable eddy activity, which arises from the convergence of SubAntarctic Water

88   (SAW) and Sub-Tropical Water (STW) (Bostock et al., 2013; Butler et al., 1992; Fernandez et

89   al., 2014). The convergence zone is locked topographically to the Chatham Rise, a shallow

90   (<300 m deep) submarine ridge, and is a region of high temperature, salinity and nutrient

91   gradients as a result of the confluence of two significantly different water masses (SAW and

92   STW) (Chiswell et al., 2015; Nodder et al., 2005). A warm core eddy immediately north of the

93   Chatham Rise is a persistent feature in the region, which extends to 2000 m depth; and has

94   been observed to have a spring bloom at its centre, which induces oligotrophic conditions in

95   summer, and is followed by deep winter mixing and low productivity in winter (Murphy et al.,

96   2001; Nodder et al., 2005). Phytoplankton community structure in the bloom is generally

97   characterised by chlorophyll (Chl) concentrations >1 mg m^{-3}, and large phytoplankton (>20

98   μm) (Boyd et al., 2012). Consequently, the area is marked by high seasonal fluxes of biogenic

99   material to deeper waters (Nodder et al., 2005; Nodder and Northcote, 2001).

100   The relatively low concentrations of $Si(OH)_4$ (~2 μmol L^{-1}) compared to NO_3^- (~4 μmol L^{-1}) in

101   surface-ocean waters testify to the influence of SAW in the region (Boyd et al., 1999). A

102   number of Fe-process studies have been undertaken in the region (e.g. (Boyd et al., 2012; Boyd

103   et al., 2015; Ellwood et al., 2015). These studies found that during the 2008 annual spring

104   bloom dissolved Fe and nutrients are sufficient to support bloom initiation, however its

105   duration and magnitude is primarily set by competition for dissolved Fe between various

106   microbe and phytoplankton groups, which ultimately limits overall production in these waters.

107   In contrast, relatively little is known on the biological fractionation of Si-isotopes by diatoms

108   in New Zealand surface waters. Instead, a majority of the processes relating to variations in

109     $\delta^{30}Si$ in $Si(OH)_4$ and diatom derived BSi in the region are inferred from previous studies in the

110   Southern Ocean and Equatorial Pacific e.g. (Beucher et al., 2008; de Souza et al., 2012a; Fripiat

111   et al., 2012). At present, the only studies investigating Si-isotopes in New Zealand waters are

112   for diatoms and sponges collected in the mesopelagic zone south of New Zealand, an area that

113   is more strongly influenced by SAW (Egan et al., 2012; Rousseau et al., 2016; Wille et al.,

114   2010).

115   The aims of the voyage were to (1) investigate the physicochemical factors driving the

116   longevity, magnitude and termination of the spring phytoplankton bloom, (2) to investigate

117   trace metal cycling within the bloom, and (3) to relate this mechanistic understanding of
118   environmental controls on bloom dynamics to remotely sensed-trends in phytoplankton blooms
119   across the mesoscale eddy field east of New Zealand (See Ellwood *et al.* 2015 and references
120   therein). The survey drew on the findings from an earlier voyage in September 2008 (FeCycle
121   II), and utilised a mesocosm experiment to investigate pelagic Fe-cycling within the resident
122   phytoplankton community (Boyd et al., 2012; Ellwood et al., 2015; Ellwood et al., 2014). The
123   work presented here is a supporting study that investigated factors driving BSi formation and
124   Si-isotope fractionation within the spring bloom in the convergence zone east of New Zealand.
125   The aim of this work was to investigate whether the fractionation of Si isotopes in subtropical
126   surface waters east of New Zealand are influence by changes in Fe bioavailability as the annual
127   spring bloom develops. To elucidate whether Fe bioavailability and phytoplankton bloom
128   development influence δ^{30}Si, we complemented water column sampling with a large mesocosm
129   (700 L) experiment and smaller (20 L) incubation experiments. Here, we present comparisons
130   of BSi production and Si-isotope (δ^{30}Si$_{BSi}$) fractionation in the mesocosm with new δ^{30}Si$_{BSi}$
131   data from the subtropical-convergence zone.

132

2. Methods

2.1 Sampling Site and Experimental Design

135   The present survey (TAN1212) was part of a GEOTRACES process study and took place in a
136   zone of confluence east of New Zealand (approximately 179ºW, 39ºS). The voyage took place
137   between 15 September 2012 (year day 259) and 7 October 2012 (year day 281). Survey
138   methods were similar to those for a previous voyage in September of 2008 (Boyd et al., 2012);
139   where after an initial survey of the eddy, a drogued drifter was deployed at the centre of the
140   eddy to provide the quasi-Lagrangian sampling platform needed to interpret biogeochemical
141   observations of the feature (for further details on eddy formation, see Boyd et al. (2012) and
142   Ellwood et al. (2014)).

143   Sea surface (0 – 10m depth) samples for BSi and Si-isotopes were collected between days 263
144   and 279 using the ships underway seawater supply. Sea surface Chl *a* fluorescence,
145   photosystem II (PSII) photochemical efficiency (F_v/F_m), and the effective absorption cross
146   section of PSII (σ_{PSII}) were monitored in real-time using a Chelsea Instruments Fast Repetition
147   Rate (FRR) fluorometer that was plumbed into the ships underway water supply. Periodically,

148   size-fractionated Chl *a* samples were collected for analysis. Daily sea-surface samples (10m

149   depth) were collected for dissolved macro-nutrients ($NO_3^- + NO_2^-$, $Si(OH)_4$ and PO_4^{3-}),

150   particulate nitrogen (PON), particulate carbon (POC), and particulate phosphorus (POP) were

151   collected off pre-dawn sampling casts utilising Niskin bottles deployed on a 24 bottle CTD

152   rosette system (SBE 911plus CTD rosette). Samples for bacteria, *Synechococcus*,

153   *Prochlorococcus*, and pico-eukaryote cell enumeration were collected using the procedures

154   described by Hall et al. (2004)

155   Daily sea-surface samples (10 m depth) for dissolved Fe (DFe) were obtained using a trace

156   metal clean (TM) rosette. Macro-nutrient concentrations were measured in real-time using a

157   micro-segmented flow analyzer (Astoria Pacific International [API300]) with digital detection

158   (Ellwood et al., 2014). Dissolved Fe (DFe) concentrations were determined onboard by flow-

159   injection analysis with chemiluminescence detection of Fe using luminol after Fe pre-

160   concentration on to Toyopearl AF-Chelate-650 M resin (de Jong et al., 1998) and spiking with

161   hydrogen peroxide (Lohan et al., 2006). Samples for DOC were analysed at the National

162   Institute of Water and Atmospheric Research (NIWA) according to APHA method 5310B

163   using a TOC analyser.

164   A mesocosm experiment was conducted on day 266 using an acid cleaned 1000 L LDPE bag

165   filled with 350 L of surface seawater that was pre-filtered using an acid cleaned 0.2 µm capsule

166   filter (Supor Acropak 200; Pall). Surface seawater was collected in a trace metal clean manner

167   using a tow fish (Ellwood et al., 2014). The main aim of the mesocosm experiment was to

168   mimic Fe cycling of pelagic Fe in the water column (see Ellwood et al. (2015) for more details).

169   Two bags were used, one spiked with 0.2 nmol L^{-1} of the radionuclide ^{55}Fe and a control, spiked

170   with 0.2 nmol L^{-1} of non-radioactive Fe. Both bags were allowed to equilibrate with natural

171   ligands present in the filtered seawater for 12 hours before being inoculated with another 350

172   L of unfiltered seawater collected using the TM tow fish containing the natural plankton

173   community (Ellwood et al., 2015). The total volume in each bag was 700 L. The bags were

174   incubated on deck for 168 hours at 50% of the ambient light intensity (attenuated with neutral

175   density screening), and kept at ambient seawater temperature by continual surface seawater

176   circulation around the bags. All analyses and observations for the work presented in this study

177   were made on the bag spiked with non-radioactive Fe. The Fe cycling results for the radioactive

178   Fe experiments are were presented by Ellwood et al. (2015).

179   To determine the influence the addition of Fe in the mesocosm might have on the resident
180   diatom community, and hence BSi production and the fractionation of $\delta^{30}Si_{BSi}$, a smaller
181   microcosm experiment was run in conjunction on day 272. The experiment was run for 96
182   hours and acted as an Fe-free control. For this experiment, four 20 L low density polyethene
183   cubic containers were filled using unfiltered seawater from the tow fish, with two of the
184   containers spiked with 0.5 nmol L^{-1} of dissolved Fe, and incubated as described for the
185   mesocosm experiment. For the mesocosm and microcosm experiments pre-incubation samples
186   were collected for macro-nutrient concentrations, BSi and Si-isotopes, photosynthetic
187   parameters (fluorescence, F_v/F_m and σ_{PSII}) and POC, PON and POP. The 700 L mesocosm
188   experiment was sampled every 12-24 hours while the 20 L microcosm experiment was only
189   sampled at the end of the 96-hour incubation in order to avoid possible Fe contamination.

190

191   *2.2 POC, PON , POP and BSi Analysis*
192   Samples for POC and PON analysis were collected by filtering between 500 and 750 mL of
193   seawater through a pre-combusted 25 mm GFF filter (Merck-Millipore), before rinsing with
194   50 ml of filtered seawater. Filters were stored at -80°C before analysis. Samples for BSi and
195   silicon isotope analysis were collected onto 25 mm 0.4 µm polycarbonate filters (Pall). Surface
196   seawater samples and samples from the mesocosm experiment were collected by filtering 30 –
197   60 L (for surface seawater) and 10 – 20 L (for mesocosm and microcosm samples) of sample,
198   respectively, through a 142 mm 0.4 µm polycarbonate filter. The filter was immediately placed
199   in a 50 ml polypropylene tube and capped. All filters were stored at -20 °C prior to analysis.
200   Hydrolysis of the samples for BSi content was carried out by adding 18 ml of 0.5% (w/w)
201   Na_2CO_3 solution to the tubes and heating them to 85 °C for 2 hr (Paasche, 1980). When cool,
202   each tube was neutralized with 0.5 M HCl to the turning point of methyl orange (pH 3–4),
203   before being made up to 25 mL with deionised water. Silicate concentrations were determined
204   using the molybdenum blue method (Strickland and Parsons, 1972).

205

206   *2.3 Preparation of samples for determination of $\delta^{30}Si$ of BSi*
207   Samples for $\delta^{30}Si_{BSi}$ determination were rinsed from their filters into 2.5 ml Teflon bombs using
208   deionised water. They were then evaporated to dryness at 50 °C in a drying oven overnight. To
209   remove any organics that may interfere with the analysis; the samples were treated with 1 mL
210   of 30% (v/v) H_2O_2 solution and refluxed for 24 hours at 70 °C on a hotplate. Following the

oxidation of organics, the lids of the Teflon bombs were removed, and the samples were left to evaporate to dryness before adding 2 mL of 0.5 M NaOH to dissolve the sample. Samples were then left to reflux for 24 hours at 50 °C. A portion of the sample was removed, neutralised and the silicate concentration determined using the molybdenum blue method (Strickland and Parsons, 1965). Prior to silicon isotope analysis, sodium was removed from the samples using cation exchange chromatography. Twelve cation exchange columns were prepared using modified polypropylene 2.5 mL Pasteur Pipettes loaded with approximately 1 ml Dowex 50W-X8 cation exchange resin (200-400 mesh). Columns were cleaned by passing 0.5 ml of 8% (v/v) hydrofluoric acid (HF) and 3x 0.75 mL of deionised water over the resin. The resin was then protonated with 3x 0.75 mL 4M HCl followed by 3x 0.75 mL deionised water rinses. Each column was loaded with 0.5 mL of sample and then rinsed with 4x 0.75 mL of deionised water to ensure the entire sample was eluted. To minimize contamination, samples were collected in vials that were cleaned using 8% (v/v) HF, before being rinsed with deionised water.

2.4 Determination of $\delta^{30}Si$ in particulate BSi

The δ^{30}Si of diatom BSi was determined according to methods developed by (Wille et al., 2010) using a multi-collector inductively coupled plasma mass spectrometer (MC-ICP-MS) (Finnigan Neptune, Germany) in medium-resolution mode. An ESI-Apex nebulizer fitted with a Teflon inlet system and a demountable torch fitted with an alumina injector was used for sample introduction. We used a standard-sample-standard bracketing technique for data acquisition and reduction (Wille et al., 2010). The δ^{30}Si signal (based on the relative abundance of ^{30}Si to ^{28}Si (^{30}Si/^{28}Si) was calculated using the following formula:

$$\delta^{30}Si = \left\lfloor \left(\frac{R_{Sample}}{R_{Std}} \right) - 1 \right\rfloor \times 1000 \qquad (1)$$

Where R_{sample} is the ^{30}Si/^{28}Si ratio of the sample and R_{Std} is the ^{30}Si/^{28}Si ratio of the in-house RC11 diatomaceous standard. Measured δ^{30}Si and the δ^{29}Si values were then converted to be relative to the NBS28 reference standard based on the daily offset between the in-house RC11 diatomaceous standard and NBS28. The overall offset between the in-house standard and the NBS28 standard was -2.28 ± 0.14 (n = 11; mean ± 2x standard deviation). Measurements of

241 sample blanks were made prior to each run to ensure that the combined blank and background

242 was <1% of the total sample signal. NBS28 and the "Diatomite" standard detailed in Reynolds

243 et al. (2007) were also prepared with each daily run, and were measured with every three

244 samples ($\leq$ 8 diatomite/NBS28 standards per daily run). The δ^{30}Si composition of the

245 "Diatomite" standard (again relative to NBS28) produced average values for δ^{29}Si of 0.73 $\pm$

246 0.11 ‰ and δ^{30}Si of 1.42 $\pm$0.17 ‰ (2 SD, n = 11), and are within the upper 90% confidence

247 range (δ^{29}Si = 0.79 ‰, δ^{30}Si = 1.54 ‰) of the modal values (δ^{29}Si = 0.66 ‰, δ^{30}Si = 1.27 ‰)

248 from inter-laboratory comparisons performed by Reynolds et al. (2007).

249

250 Sample δ^{30}Si and the δ^{29}Si values were plotted against each other to ascertain the best-fit mass-

251 dependent fractionation line (MDF, Figure 1). Our calculated slope for the best-fit MDF line

252 was 0.55 with a regression error of 0.13 (2SE, *n* = 11) and is consistent with the consensus

253 slope of 0.511 obtained from inter-laboratory silicon standard measurements (Figure 1). This

254 value agrees with the slope of the theoretical fractionation line for Si of 0.5092 (Reynolds et

255 al., 2007).

256 Silicon isotope fractionation in diatoms has been modelled using both closed and open

257 steady-state models (Cardinal et al., 2007; De La Rocha et al., 1997; Varela et al., 2004). The

258 closed system model is employed when there is no net import or export of Si(OH)$_4$ or BSi out

259 of surface waters during the period of biological incorporation of Si (Varela et al., 2004); for

260 example, during periods of intense water column stratification where mixing across the

261 density interface separating the surface mixed layer from deeper waters is minimal

262 (Brzezinski et al., 2001). Because the mesocosm experiment has no inputs or outputs, a

263 closed system model can be used to define the evolution of δ^{30}Si through the following

264 relationships:

265 $$\delta^{30}Si(OH)_4 = \delta^{30}Si(OH)_{4\,initial} + \varepsilon\ln f \qquad (2)$$

266 $$\delta^{30}Si_{BSi.inst} = \delta^{30}Si(OH)_4 + \varepsilon \qquad (3)$$

267 $$\delta^{30}Si_{BSi.acc} = \delta^{30}Si(OH)_{4\,initial} - \varepsilon(f\ln f/1-f) \qquad (4)$$

268 Where δ^{30}Si(OH)$_4$ is the isotopic composition of Si(OH)$_4$ in seawater, δ^{30}Si(OH)$_{4initial}$ is the

269 initial isotopic composition of Si(OH)$_4$ in seawater prior to biological incorporation of Si(OH)$_4$,

270 δ^{30}BSi$_{inst}$ and δ^{30}BSi$_{acc}$ are the instantaneous BSi product and accumulated BSi product

271   (respectively), and f is the fraction of $Si(OH)_4$ remaining in the system after BSi formation

272   ($[Si(OH)_4]/[Si(OH)_{4initial}]$) (Varela et al., 2004). The Rayleigh isotope fractionation model

273   assumes a constant value for α (the fractionation factor), also known as the enrichment factor

274   (ε), where ε (‰) $\approx (1 - \alpha) \times 1000$.

275

3. Results

3.1 Surface water data

Phytoplankton bloom initiation commenced with a shoaling of the mixed layer on day 272 and continued until the end of the voyage on day 279, with surface fluorescence (Arbitrary units, AU) ranging from < 0.5 prior to bloom formation, to 1.0 after the bloom (Figure 2A). Nitrate and DFe concentrations exhibit 1.5 – 3 fold decreases in surface concentrations during bloom initiation (Figures 2B, 3 and 4A), with NO_3^- concentrations decreasing from >4.8 μmol L^{-1} on day 267 to < 2.3 μmol L^{-1} on day 278, and DFe concentrations decreasing from > 0.3 nmol L^{-1} on day 267 to < 0.2 nmol L^{-1} on days 278 and 279. Silicic acid concentrations were relatively low (< 2 μmol L^{-1}) in comparison to NO_3^- (≤ 5 μmol L^{-1}) during the voyage and exhibited little variation during bloom initiation (Figure 4A).

From the start of the voyage, the phytoplankton community composition in surface waters was dominated by eukaryotic pico-phytoplankton (0.2 – 2 μm in size) and prokaryote pico-phytoplankton (*Synechococcus* and *Prochlorococcus*) (Figure 4B). Pico-eukaryotic plankton cell numbers increased relative to the other plankton groups, exhibiting a 2-fold increase on day 270 and a 3-fold increase by day 279. In comparison, both *Synechococcus* and *Prochlorococcus* populations exhibit little variation between days 263 and 273. *Synechococcus* and *Prochlorococcus* populations change rapidly, however, following day 273, where they exhibit 5-fold and 8-fold increases in their respective populations between days 273 and 279. The pico-phytoplankton also dominated the Chl *a* estimates of phytoplankton biomass (Figure 4D). Night-time measurements of F_v/F_m average around 0.4 between days 263 and 272 before dropping to around 0.3 by day 274 (Figure 4B), following the decline in dissolved Fe concentration (Figure 4A). Between days 274 and 278, F_v/F_m remained around 0.3.

Surface elemental ratios and POC, PON and BSi concentrations are presented in Figure 4, while surface values for $\delta^{30}Si$ from BSi are presented in Table 1. BSi concentrations remained consistent at 0.07 ± 0.02 μmol L^{-1} for the duration of the voyage and displayed little variation despite a relative increase in concentration at the onset of the bloom, from 0.049 μmol L^{-1} on day 273 to 0.103 μmol L^{-1} on day 276 (Table 1, Figure 4C). The lack of variation in surface BSi is reflected in the relatively small change in surface $Si(OH)_4$ concentrations over the duration of the voyage (Figure 4A). Particulate organic nitrogen exhibits a 2-fold increase on day 273 (Figure 4C), which is concomitant with a relative decrease in the surface NO_3^- concentration of ~1.3 μmol L^{-1} (Figure 4A). Samples for $\delta^{30}Si_{BSi}$ from BSi were taken

11

308   prior to bloom initiation on days 268 and 270 and exhibited $\delta^{30}Si_{BSi}$ values of 1.61 ± 0.2 ‰

309   and 1.83 ± 0.2 ‰, respectively (Figure 2B, Table 1), whereas $\delta^{30}Si_{BSi}$ values were relatively

310   lighter with respect to ^{30}Si following bloom initiation, with $\delta^{30}Si_{BSi}$ values of 1.35 ± 0.2 ‰ on

311   day 275, and 1.22 ± 0.2 ‰ on day 279, respectively.

312   *3.2. Mesocosm (700 L bag) experiment*

313   There was a significantly different response in the mesocosm experiment compared to the

314   response in surface waters over the duration of the voyage. Fluorescence and F_v/F_m increased

315   with peak fluorescence at around 160 hr (Table 2 Figure 5A). BSi, NO_3^- and $Si(OH)_4$

316   concentrations in the bag at the start of the experiment were comparable to sea-surface

317   concentrations of BSi, NO_3^- and $Si(OH)_4$ on day 266, when the experiment was initiated. Both

318   NO_3^- and $Si(OH)_4$ concentrations exhibited an 11-fold and 9-fold decrease (respectively) by the

319   end of the mesocosm experiment, while BSi concentrations increased from 0.1 $\mu mol\ L^{-1}$ to 1.3

320    $\mu mol\ L^{-1}$ by the end of the mesocosm experiment (Figure 5B). There was almost complete

321   utilisation of the $Si(OH)_4$ pool in the mesocosm by siliceous organisms, with BSi production

322   reaching $18 \pm 1\ nmol\ L^{-1}\ hr^{-1}$ during the exponential phase of growth. This value closely

323   resembles the rate of $Si(OH)_4$ depletion in the mesocosm, which reached $20 \pm 1\ nmol\ L^{-1}\ hr^{-1}$

324   during the exponential phase of growth.

325   The starting value $\delta^{30}Si_{BSi}$ for BSi in the mesocosm experiment was 1.49 ± 0.2 ‰ (t = 0 hr)

326   and comparable to the sea-surface $\delta^{30}Si_{BSi}$ value of 1.61 ± 0.2 ‰ collected on day 268 (Figure

327   5B). Over the course of the mesocosm experiment, $\delta^{30}Si_{BSi}$ values became heavier with respect

328   to ^{30}Si, with $\delta^{30}Si_{BSi}$ values increasing to 2.64 ± 0.2 ‰ by the end of the experiment (Figure

329   5B). Silicon isotope fractionation within the experiment closely resembled Rayleigh

330   fractionation kinetics, and a fractionation factor (α) of 0.9989, and an initial $\delta^{30}Si_{DSi}$ value of

331   2.92 ± 0.1 ‰ was calculated by fitting a model to the $\delta^{30}Si_{BSi}$ for BSi (Figure 5C) (De La Rocha

332   et al., 1997). While no phytoplankton community data were available for the mesocosm

333   experiment, examination of late exponential populations confirmed the presence of the diatoms

334   *Asterionelopsis glacilis*, *Mellosira moniliformis* and *Ceratium arcticum* (Figure 6).

335   *3.3.Microcosm (20 L) experiment*

336   Derived photosynthetic parameters from the microcosm experiment are presented in Figure 7.

337   Despite the increase in Chl *a* fluorescence at the end of the experimental period in both control

338   and Fe-addition experiments, both F_v/F_m and Chl *a* concentration decreased in the control

339   experiment, whilst Chl *a* concentration and F_v/F_m increased ($p < 0.05$) in response to Fe-

340 addition (Figure 7A, Table 3). The PSII effective absorption cross-section (σ_{PSII}) decreased in

341 both treatments by the end of the experimental period, however, this decrease was more

342 pronounced in the Fe-addition experiment. BSi concentration increased from 0.1 μmol L^{-1} at

343 T=0 to 0.9 ±0.2 μmol L^{-1} and 1.1 ±0.1 μmol L^{-1} at T=96 in the control and Fe-addition

344 experiments, respectively. The increase in BSi concentration is consistent with the mesocosm

345 (700 L bag experiment, Figure 7) which exhibited a 12-fold increase in BSi concentration at

346 the end of the experimental period. In addition, both POC and PON concentrations exhibited a

347 2 – 3 fold increase at the end of the experimental period (Figure 7B), with POC responding

348 more strongly to Fe-addition in comparison to the control experiment. As a result, both

349 treatments exhibited significant increases in elemental ratios at the end of the experimental

350 period (Figure 7C). The increase in the C:N ratio, however, was more pronounced in the Fe-

351 addition treatment, where POC concentration increased 3-fold compared to a 2.4-fold increase

352 in the control. Increases in Si:N and Si:C ratios were due to a more pronounced increase in BSi

353 concentrations compared to increases in PON and POC concentrations. The addition of

354 dissolved Fe appeared had little effect ($p > 0.1$) on the Si:N and Si:C ratios at the end of the

355 experimental period (Figure 7C).

356

4. Discussion

Here we first discuss the silicic acid, BSi and silicon isotope results from the mesocosm and microcosm experiments. We then place the experiments into context by comparing the findings with water column measurements. We then detail the processes that might regulate silicic acid utilisation in the waters east of New Zealand.

The fractionation of Si isotopes in the mesocosm bag experiment closely resembled Rayleigh fractionation closed-system kinetics as $Si(OH)_4$ was drawdown (Figure 5B). BSi concentration increased 12-fold in the mesocosm over 8 days resultant from increased in diatoms production thus leading to an increase in $\delta^{30}Si_{BSi}$. The value for $\delta^{30}Si_{BSi}$ at the beginning of the mesocosm experiment was 1.49 ± 0.2 ‰, which closely resembled surface values for $\delta^{30}Si_{BSi}$ measured prior to bloom initiation on days 268 and 270 (Figure 5, Table 1). As the experiment progressed $\delta^{30}Si_{BSi}$ increased to 2.64 ± 0.2 ‰ by the end of the experiment. Based on the increase in $\delta^{30}Si_{BSi}$ and the drawdown in silicic acid as the mesocosm bag experiment progressed, we were able to calculate a fractionation factor (α) of 0.9989 (ε = -1.1 ‰) and a starting seawater value for $\delta^{30}Si_{DSi}$ of 2.92 ± 0.1 ‰. The fractionation factor reported from the mesocosm experiment closely resembles fractionation factors previously published for laboratory and field communities. De La Rocha et al. (1997) obtained a value for ε of -1.1 ± 0.4 ‰ for the diatoms *Thalassiosira weisfloggii*, *Thalassiosira sp.* and *Skeletonema costatum* cultured in the laboratory and found that fractionation was independent of species or temperature. More recently Sutton et al. (2013), however, found significant variations in ε between the Southern Ocean species *Chaetoceros brevis* (-2.09 ± 0.09 ‰) and *Fragilariopsis kergulensis* (-0.56 ± 0.07 ‰)., The fractionation factor reported here (-1.13 ± 0.1 ‰) from the mesocosm experiment also closely resembles fractionation factors reported for field communities, e.g. Varela et al. (2004)(-1.2 ±0.2 ‰), Fripiat et al. (2011)(−1.0 ± 0.3‰) suggesting that species composition of the overall diatom community in the open ocean plays an important role in governing the Si isotope composition in surface waters.

The high $\delta^{30}Si_{DSi}$ value calculated from the mesocosm experiment reflects the relatively high $\delta^{30}Si_{BSi}$ values observed at the start of the experiment and also reflects the surface water composition prior to bloom initiation on days 268 and 270 (Figure 5, Table 1). The calculated $\delta^{30}Si_{DSi}$ of 2.92 ± 0.1 ‰ from the experiment is within the range expected for sub-tropical and tropical water (Beucher et al., 2008) and matches those reported from the Polar Frontal Zone of the Pacific Sector of the Southern Ocean (~3.2 ‰) (de Souza et al., 2012b).

389 In contrast to the mesocosm experiment, changes to Si(OH)$_4$ and BSi concentrations for surface

390 waters within the eddy were relatively subtle (Figure 2B). In contrast to mesocosm experiment,

391 sea-surface values for $\delta^{30}Si_{BSi}$ were relatively constant between days 268 and 270 and then

392 decline by about ~0.5 ‰ though to day 279, following bloom initiation (Table 1). The surface

393 water values presented here on days 275 and 279 for $\delta^{30}Si_{BSi}$ resemble values reported for

394 waters north of the Sub-tropical front in the Atlantic sector of the Southern Ocean (1.30 ± 0.1

395 ‰)(Fripiat et al., 2012). It is likely that the observed shift in the $\delta^{30}Si_{BSi}$ composition in surface

396 waters towards lighter Si isotopes could be attributable to a change in the supply of Si(OH)$_4$ to

397 surface waters, possibly from SAW (Figure 2B). It also reflects the open system nature of the

398 area.

399 In contrast to the mesoscom experiment the BSi concentration in surface waters varied little

400 during the ~17 day voyage, only increasing from 0.05 μmol L^{-1} on Day 264 to 0.11 μmol L^{-1}

401 on day 278 (Figure 4C). The relatively rapid uptake of Si(OH)$_4$ in the mesocosm experiment

402 as well as the 12-fold increase in BSi concentrations, in contrast to lack of *in situ* BSi

403 production, suggest that changes in water-column stability may have encouraged more rapid

404 bloom initiation compared to surface waters. It is possible that Fe had a small stimulatory effect

405 within the mesocosm experiment, although it was only increased by 0.2 nmol L^{-1} relative to

406 surface waters, which were 0.3-0.4 nmol L^{-1}. This was tested in smaller microcosm (20 L)

407 experiments, where the rate of BSi production show little variation between control and Fe-

408 addition replicates ($p > 0.05$). In these smaller experiments, Fe addition did seem to affect

409 photosynthetic parameters (F_v/F_m, σ_{PSII} and Chl *a* fluorescence) as well as POC concentration

410 in comparison to the control experiment such that some community dynamics may have

411 differed in the mesocosm experiment compared to the community in surface waters. It is

412 possible that the small addition of Fe may have removed resource competition between diatoms

413 and other phytoplankton in the mesocosm experiment, however, it is more likely that the larger

414 phytoplankton were initially dominating before being run into nitrate and possibly Fe-

415 limitation (Boyd et al., 2012; Ellwood et al., 2015; Ellwood et al., 2014).

416 The surface water plankton community was dominated by the presence of eukaryotic

417 picoplankton (0.2 – 2 μm), and a background population of photosynthetic prokaryotes

418 (*Synechococcus* and *Prochlorococcus*). Size-fractionated Chl *a* distribution suggests that the

419 picoplankton community dominated photosynthetic biomass. Previous studies in the area also

420 suggest that at its peak, the phytoplankton bloom is dominated by photosynthetic prokaryotes

421 and large diatoms such as *Asterionellopsis glacilalis* (cell volume ~ 60 μm^3) and

422 *Leptocylindrus sp.* (~ 600 μm^3) (Boyd et al., 2012). Similarly, we observed an increased

423 abundance of *A. glacialis*, *M. moniliformis* and *C. arcticum* in the exponential stage population

424 in the mesocosm experiment, but not for our water column measurements.

425 At this stage it is difficult to determine why $Si(OH)_4$ was depleted in the mesocosm, whilst the

426 sea-surface inventory was maintained. The consumption of $Si(OH)_4$ and the formation of BSi

427 in the mesocosm experiment suggests that $Si(OH)_4$ is not the ultimate factor limiting diatom

428 productivity as the water column stratifies and the spring bloom progresses (Boyd et al., 2012).

429 Ultimately the lack of bloom formation in the present study is likely due to water column

430 instability and unfavourable Fe and light supply conditions for bloom initiation (Chiswell et al.

431 submitted), as well as a dominant diatom phytoplankton assemblage compared to picoplankton.

432 Zooplankton grazing may also be suppressed in the mesocosm experiment, which may allow

433 full nutrient and Fe consumption, although during spring bloom development primary

434 producers tend to outcompete grazers (Boyd et al., 2012). For the current study, a fully

435 developed spring bloom did not occur at this site, even after the voyage was competed

436 (Chiswell et al. submitted); there is a hint of a potential iron limitation of the plankton

437 community whereby F_v/F_m declined from 0.4 to 0.3 following a decline in dissolved Fe

438 concentration (Figure 4), so perhaps this was contributing factor to the lack of bloom

439 development.

440 One of the more important findings of the study was that despite the large species-level

441 variability in Si isotope fractionation factors observed by Sutton et al. (2013), the community

442 level fractionation factor of -1.1 ‰ determined in in this study agrees well with previous

443 estimates of -1.2 ‰ (observed by Fripiat et al. 2012), and -1.1 ‰ (observed by De la Rocha et

444 al. 1997). Furthermore, the fractionation factor that was obtained from the mesocosm

445 experiment appears to exhibit little variation despite the relatively low ambient $Si(OH)_4$

446 concentrations of 2 $\mu mol\ L^{-1}$ (compared to the Southern Ocean waters, where Si concentrations

447 can be >20 $\mu mol\ L^{-1}$) (de Souza et al., 2012b; Frank et al., 2003). This highlights the utility of

448 the diatom $\delta^{30}Si$ as a proxy for diatom $Si(OH)_4$ utilisation in paleo-reconstructions (e.g.

449 Beucher et al., 2007; De La Rocha et al., 1998) and that species level variation in Si isotope

450 fractionation may not be important when considering past trends in diatom $Si(OH)_4$ utilisation.

451

452

4.3. Conclusions

Contrasting results between the mesocosm (700 L) bag experiment and sea-surface measurements suggest that $\delta^{30}Si_{BSi}$ in surface waters rarely exceeds ~ 2 ‰ as a result of Fe-limitation of the diatom population at the end of a phytoplankton bloom (Boyd et al., 2012); and the continuous re-supply of $Si(OH)_4$ to surface waters. Despite this, $\delta^{30}Si_{DSi}$ values in subtropical surface waters east of New Zealand are relatively high, and it is likely that silicic acid resupply by waters enriched in ^{30}Si likely plays a larger role in governing the $\delta^{30}Si$ composition of surface waters, in addition to biological fractionation by diatoms. We also observed that the community level Si isotope fractionation factor is independent of species composition and $Si(OH)_4$ concentration. Our observed value of -1.1 ‰ is also consistent with previous field studies (Fripiat et al. 2012 and Varela et al. 1997) and similar to mono-specific lab culture studies (De la Rocha et al. 1997 and Milligan et al. 2004).

473 **Table 1.** Surface BSi concentrations and δ^{30}BSi values over the duration of the voyage. Duplicate
474 samples for BSi were taken on days 266, 268 and 270 (mean ± 1 SD). δ^{29}Si$_{BSi}$ and δ^{30}Si$_{BSi}$ values are
475 per mil (‰) with errors based on 2 standard deviation calculated from multiple measurements.

Longitude/Latitude	Day	Date	δ^{29}Si$_{BSi}$	δ^{30}Si$_{BSi}$	Surface BSi concentration (μmol L^{-1})
179.14 W 39.09 S	263	19/09/2012			0.092
179.15 W 39.07 S	264	20/09/2012			0.084
179.15 W 39.07 S	265	21/09/2012			0.074
179.17 W 39.02 S	266	22/09/2012			0.091 ± 0.050
179.24 W 38.58 S	267	23/09/2012			0.055
179.29 W 38.58 S	268	24/09/2012	0.82 ± 017	1.61 ± 0.25	0.073 ± 0.010
179.30 W 38.58 S	269	25/09/2012			0.040
179.27 W 39.10 S	270	26/09/2012	0.96 ± 0.17	1.83 ± 0.25	0.071 ± 0.010
179.34 W 38.50 S	271	27/09/2012			0.056
179.40 W 38.52 S	272	28/09/2012			0.049
179.40 W 39.04 S	273	29/09/2012			0.049
179.38 W 38.52 S	274	30/09/2012			0.046
179.56 W 38.28 S	275	01/10/2012	0.66 ± 0.17	1.35 ± 0.25	0.045
179.53 W 38.28 S	276	02/10/2012			0.102
179.58 W 38.59 S	277	03/10/2012			0.088
179.45 W 39.04 S	278	04/10/2012			0.110
179.49 W 38.60 S	279	05/10/2012	0.60 ± 0.17	1.22 ± 0.25	0.092

476

477

478   **Table 2.** Results from the mesocosm (700 L bag) experiment for BSi, NO_3^- and $Si(OH)_4$, the isotope

479   composition ($\delta^{30}Si_{BSi}$) of BSi, fluorescence, and F_v/F_m.

Time (hr)	BSi (µmol L^{-1})	$\delta^{30}Si_{BSi}$ (‰)	Si(OH)$_4$ (µmol L^{-1})	NO$_3$ (µmol L^{-1})	F$_o$	F$_v$/F$_m$
0	0.091	1.49			2.40	0.06
22					1.90	0.19
24	0.042	1.62	1.88	4.78		
36	0.049	1.94				
38			1.94	4.77		
46					1.80	0.23
48	0.087					
51			1.95	4.70		
58					2.00	0.23
61			1.87	4.58		
72	0.157				2.30	0.23
75			1.81	4.44		
94					3.20	0.35
96	0.332	2.04				
98			1.74	3.53		
118					7.10	0.36
120	0.542	2.19				
122			1.16	2.50		
144	0.750	2.54			12.8	0.26
146			0.82	1.55		
166					13.2	0.27
168	1.29	2.64				
170			0.47	0.42		
190					12.8	0.24
194			0.28			

480

481 **Table 3.** Values from microcosm (20 L) experiment at T = 0 hours and at T = 96 hours (n ≥ 3, 1 S.D).
482 BSi, Si:N and Si:C values with no error (*) reflect the single BSi measurement taken at T= 0 hours
483 prior to the start of the experiment.

Parameter	T = 0 hr	Control (T = 96 hr)	Fe-addition (T = 96 hr)
Chl *a* fluorescence	3.95 ±0.1	9.12 ±0.4	8.62 ±0.5
F_v/F_m	0.38 ±0.02	0.35 ±0.01	0.41 ±0.01[*]
σPSII	762 ±61	717 ±35	595 ±41[*]
Chl a (mg L^{-1})	1.34 ±0.1	1.26 ±0.1	1.75 ±0.1[†]
POC (µmol L^{-1})	10.2 ±0.5	24.7 ±1.1	31.6 ±2.5[†]
PON (µmol L^{-1})	1.6 ±0.01	3.24 ±0.2	3.22 ±0.2
BSi (µmol L^{-1})	0.1[*]	0.92 ±0.2	1.09 ±0.1
Si:N (mol/mol)	0.06[*]	0.28 ±0.05	0.34 ±0.03
Si:C (mol/mol)	0.01[*]	0.04 ±0.001	0.03 ±0.004
C:N (mol/mol)	6.38 ±0.23	7.64 ±0.09	9.8 ±0.18[‡]

484 [*]Variation from control at the 90-95 % confidence interval

485 [†]Variation from control at the 95-99% confidence interval

486 [‡]Variation from control at >99% confidence interval

References

Baines, S.B., Pace, M.L., 1991. The production of dissolved organic matter by phytoplankton and its importance to bacteria: Patterns across marine and freshwater systems. Limnology and Oceanography 36, 1078-1090.

Beucher, C.P., Brzezinski, M.A., Jones, J.L., 2008. Sources and biological fractionation of Silicon isotopes in the Eastern Equatorial Pacific. Geochim. Cosmochim. Acta 72, 3063-3073.

Bostock, H.C., Sutton, P.J., Williams, M.J.M., Opdyke, B.N., 2013. Reviewing the circulation and mixing of Antarctic Intermediate Water in the South Pacific using evidence from geochemical tracers and Argo float trajectories. Deep-Sea Research Part I: Oceanographic Research Papers 73, 84-98.

Boyd, P., LaRoche, J., Gall, M., Frew, R., McKay, R.M.L., 1999. Role of iron, light, and silicate in controlling algal biomass in subantarctic waters SE of New Zealand. Journal of Geophysical Research-Oceans 104, 13395-13408.

Boyd, P.W., Strzepek, R., Chiswell, S., Chang, H., DeBruyn, J.M., Ellwood, M., Keenan, S., King, A.L., Maas, E.W., Nodder, S., Sander, S.G., Sutton, P., Twining, B.S., Wilhelm, S.W., Hutchins, D.A., 2012. Microbial control of diatom bloom dynamics in the open ocean. Geophys. Res. Lett. 39, L18601.

Boyd, P.W., Strzepek, R.F., Ellwood, M.J., Hutchins, D.A., Nodder, S.D., Twining, B.S., Wilhelm, S.W., 2015. Why are biotic iron pools uniform across high- and low-iron pelagic ecosystems? Global Biogeochemical Cycles 29, 1028–1043.

Brzezinski, M.A., Dumousseaud, C., Krause, J.W., Measures, C.I., Nelson, D.M., 2008. Iron and silicic acid concentrations together regulate Si uptake in the equatorial Pacific Ocean. Limnology and Oceanography 53, 875-889.

Brzezinski, M.A., Nelson, D.M., Franck, V.M., Sigmon, D.E., 2001. Silicon dynamics within an intense open-ocean diatom bloom in the Pacific sector of the Southern Ocean. Deep Sea Res. Pt II 48, 3997-4018.

Brzezinski, M.A., Pride, C.J., Franck, V.M., Sigman, D.M., Sarmiento, J.L., Matsumoto, K., Gruber, N., Rau, G.H., Coale, K.H., 2002. A switch from $Si(OH)_4$ to NO_3^- depletion in the glacial Southern Ocean. Geophys. Res. Lett. 29, doi:10.1029/2001GL014349.

Butler, E.C.V., Butt, J.A., Lindstrom, E.J., Tildesley, P.C., Pickmere, S., Vincent, W.F., 1992. Oceanography of the subtropical convergence zone around Southern New Zealand. New Zealand Journal of Marine and Freshwater Research 26, 131-154.

Cardinal, D., Savoye, N., Trull, T.W., Dehairs, F., Kopczynska, E.E., Fripiat, F., Tison, J.-L., Andre, L., 2007. Silicon isotopes in spring Southern Ocean diatoms: Large zonal changes despite homogeneity among size fractions. Marine Chemistry 106, 46-62.

Chiswell, S.M., Bostock, H.C., Sutton, P.J.H., Williams, M.J.M., 2015. Physical oceanography of the deep seas around New Zealand: a review. New Zealand Journal of Marine and Freshwater Research, 1-32.

de Jong, J.T.M., den Das, J., Bathmann, U., Stoll, M.H.C., Kattner, G., Nolting, R.F., de Baar, H.J.W., 1998. Dissolved iron at subnanomolar levels in the Southern Ocean as determined by ship-board analysis. Analytica Chimica Acta 377, 113-124.

De La Rocha, C.L., Brzezinski, M.A., DeNiro, M.J., 1997. Fractionation of silicon isotopes by marine diatoms during biogenic silica formation. Geochim. Cosmochim. Acta 61, 5051-5056.

de Souza, G.F., Reynolds, B.C., Johnson, G.C., Bullister, J.L., Bourdon, B., 2012a. Silicon stable isotope distribution traces Southern Ocean export of Si to the eastern South Pacific thermocline. Biogeosciences 9, 4199–4213.

535   de Souza, G.F., Reynolds, B.C., Rickli, J., Frank, M., Saito, M.A., Gerringa, L.J.A., Bourdon,
536   B., 2012b. Southern Ocean control of silicon stable isotope distribution in the deep Atlantic
537   Ocean. Global Biogeochem. Cycles 26, GB2035.
538   Egan, K.E., Rickaby, R.E.M., Leng, M.J., Hendry, K.R., Hermoso, M., Sloane, H.J., Bostock,
539   H., Halliday, A.N., 2012. Diatom silicon isotopes as a proxy for silicic acid utilisation: A
540   Southern Ocean core top calibration. Geochim. Cosmochim. Acta 96, 174-192.
541   Ellwood, M.J., Hutchins, D.A., Lohan, M.C., Milne, A., Nasemann, P., Nodder, S.D., Sander,
542   S.G., Strzepek, R., Wilhelm, S.W., Boyd, P.W., 2015. Iron stable isotopes track pelagic iron
543   cycling during a subtropical phytoplankton bloom. Proceedings of the National Academy of
544   Sciences 112, E15-E20.
545   Ellwood, M.J., Nodder, S.D., King, A., Hutchins, D.A., Wilhelm, S.W., Boyd, P.W., 2014.
546   Pelagic iron cycling during the subtropical spring bloom, east of New Zealand. Marine
547   Chemistry 160, 18-33.
548   Fernandez, D., Bowen, M., Carter, L., 2014. Intensification and variability of the confluence
549   of subtropical and subantarctic boundary currents east of New Zealand. Journal of
550   Geophysical Research: Oceans 119, 1146-1160.
551   Franck, V.M., Bruland, K.W., Hutchins, D.A., Brzezinski, M.A., 2003. Iron and zinc effects
552   on silicic acid and nitrate uptake kinetics in three high-nutrient, low-chlorophyll (HNLC)
553   regions. Marine Ecology Progress Series 252, 15-33.
554   Fripiat, F., Cavagna, A.-J., Savoye, N., Dehairs, F., André, L., Cardinal, D., 2011. Isotopic
555   constraints on the Si-biogeochemical cycle of the Antarctic Zone in the Kerguelen area
556   (KEOPS). Marine Chemistry 123, 11-22.
557   Fripiat, F., Cavagna, A.J., Dehairs, F., de Brauwere, A., André, L., Cardinal, D., 2012.
558   Processes controlling the Si-isotopic composition in the Southern Ocean and application for
559   paleoceanography. Biogeosciences 9, 2443-2457.
560   Hall, J.A., Safi, K., Cumming, A., 2004. Role of microzooplankton grazers in the subtropical
561   and subantarctic waters east of New Zealand. New Zealand Journal of Marine and Freshwater
562   Research 38, 91-101.
563   Lohan, M.C., Aguilar-Islas, A.M., Bruland, K.W., 2006. Direct determination of iron in
564   acidified (pH 1.7) seawater samples by flow injection analysis with catalytic
565   spectrophotometric detection: Application and intercomparison. Limnology and
566   Oceanography: Methods 4, 164-171.
567   Marchetti, A., Varela, D.E., Lance, V.P., Johnson, Z., Palmucci, M., Giordano, M., Armbrust,
568   E.V., 2010. Iron and silicic acid effects on phytoplankton productivity, diversity, and
569   chemical composition in the central equatorial Pacific Ocean. Limnology and Oceanography
570   55, 11.
571   Meyerink, S., Ellwood, M.J., Maher, W.A., Strzepek, R., 2017. Iron Availability Influences
572   Silicon Isotope Fractionation in Two Southern Ocean Diatoms (Proboscia inermis and
573   Eucampia antarctica) and a Coastal Diatom (Thalassiosira pseudonana). Frontiers in Marine
574   Science 4.
575   Milligan, A.J., Varela, D.E., Brzezinski, M.A., Morel, F.M.M., 2004. Dynamics of silicon
576   metabolism and silicon isotopic discrimination in a marine diatom as a function of pCO$_2$.
577   Limnology and Oceanography 49, 322-329.
578   Murphy, R.J., Pinkerton, M.H., Richardson, K.M., Bradford-Grieve, J.M., Boyd, P.W., 2001.
579   Phytoplankton distributions around New Zealand derived from SeaWiFS remotely-sensed
580   ocean colour data. New Zealand Journal of Marine and Freshwater Research 35, 343-362.
581   Nodder, S.D., Boyd, P.W., Chiswell, S.M., Pinkerton, M.H., Bradford-Grieve, J.M., Greig,
582   M.J.N., 2005. Temporal coupling between surface and deep ocean biogeochemical processes
583   in contrasting subtropical and subantarctic water masses, southwest Pacific Ocean. Journal of
584   Geophysical Research-Oceans 110.

585 Nodder, S.D., Northcote, L.C., 2001. Episodic particulate fluxes at southern temperate mid-
586 latitudes (42-45 degrees S) in the Subtropical Front region, east of New Zealand. Deep-Sea
587 Research Part I-Oceanographic Research Papers 48, 833-864.
588 Paasche, E., 1980. Silicon content of five marine plankton diatom species measured with a
589 rapid filter method. Limnol. Oceanogr 25, 474-480.
590 Pichevin, L.E., Ganeshram, R.S., Geibert, W., Thunell, R., Hinton, R., 2014. Silica burial
591 enhanced by iron limitation in oceanic upwelling margins. Nature Geosci 7, 541-546.
592 Reynolds, B.C., Aggarwal, J., André, L., Baxter, D., Beucher, C., Brzezinski, M.A.,
593 Engström, E., Georg, R.B., Land, M., Leng, M.J., Opfergelt, S., Rodushkin, I., Sloane, H.J.,
594 van den Boorn, S.H.J.M., Vroon, P.Z., Cardinal, D., 2007. An inter-laboratory comparison of
595 Si isotope reference materials. Journal of Analytical Atomic Spectrometry 22, 561-568.
596 Rousseau, J., Ellwood, M.J., Bostock, H., Neil, H., 2016. Estimates of late Quaternary mode
597 and intermediate water silicic acid concentration in the Pacific Southern Ocean. Earth and
598 Planetary Science Letters 439, 101-108.
599 Sarmiento, J.L., Gruber, N., Brzezinski, M.A., Dunne, J.P., 2004. High-latitude controls of
600 thermocline nutrients and low latitude biological productivity. Nature 427, 56-60.
601 Sarmiento, J.L., Simeon, J., Gnanadesikan, A., Gruber, N., Key, R.M., Schlitzer, R., 2007.
602 Deep ocean biogeochemistry of silicic acid and nitrate. Global Biogeochemical Cycles 21,
603 doi:10.1029/2006GB002720.
604 Smetacek, V., Assmy, P., Henjes, J., 2004. The role of grazing in structuring Southern Ocean
605 pelagic ecosystems and biogeochemical cycles. Antarctic Science 16, 541-558.
606 Strickland, J.D., Parsons, T.R., 1972. A practical handbook of seawater analysis.
607 Strickland, J.D.H., Parsons, T.R., 1965. A manual of sea water analysis.
608 Sutton, J.N., André, L., Cardinal, D., Conley, D.J., de Souza, G.F., Dean, J., Dodd, J., Ehlert,
609 C., Ellwood, M.J., Frings, P.J., Grasse, P., Hendry, K., Leng, M.J., Michalopoulos, P.,
610 Panizzo, V.N., Swann, G.E.A., 2018. A Review of the Stable Isotope Bio-geochemistry of
611 the Global Silicon Cycle and Its Associated Trace Elements. Frontiers in Earth Science 5.
612 Sutton, J.N., Varela, D.E., Brzezinski, M.A., Beucher, C.P., 2013. Species-dependent silicon
613 isotope fractionation by marine diatoms. Geochim. Cosmochim. Acta 104, 300-309.
614 Varela, D.E., Pride, C.J., Brzezinski, M.A., 2004. Biological fractionation of silicon isotopes
615 in Southern Ocean surface waters. Global Biogeochemical Cycles 18,
616 doi:10.1029/2003GB002140.
617 Wille, M., Sutton, J., Ellwood, M.J., Sambridge, M., Maher, W., Eggins, S., Kelly, M., 2010.
618 Silicon isotopic fractionation in marine sponges: A new model for understanding silicon
619 isotopic variations in sponges. Earth and Planetary Science Letters 292, 281-289.

620

Figures

622 **Figure 1.** Mass dependent fractionation (MDF) of $\delta^{29}Si$ vs $\delta^{30}Si$ line for all diatom samples relative to

623 NBS28. MDF line represented by $\delta^{29}Si = 0.55 \pm 0.02[\delta^{30}Si] - 0.08 \pm 0.04$, $r^2 = 0$.

624 **Figure 2. A.** Underway surface Chlorophyll fluorescence data, measured in arbitrary units (AU)

625 obtained from the FRR (Fast Repetition Rate) Fluorometer for year days 268, 270, 275 and 279 of the

626 voyage. Black dots represent drogue drifter tracks. **B**. Surface (0 - 10m) values for BSi, $Si(OH)_4$, $\delta^{30}Si$

627 and DFe for year days 268, 270, 275 and 279.

628 **Figure 3.** Profiles of DFe, $Si(OH)_4$, NO_3^-, and PO_4^{3-} concentration versus depth for year days 267,

629 270, 275 and 278.

630 **Figure 4.** A Mean surface (0 – 10 m) nutrients ($Si(OH)_4$, NO_3^-, PO_4^{3-} and DFe) over the duration

631 survey. B. cell counts for cyanobacteria and size fractionated eukaryotic phytoplankton along with

632 night-time F_v/F_m measurements. C. Concentrations of POC, PON and BSi. D. Size fractionated

633 Chlorophyll *a* concentrations and the Chl:C ratio. For surface macro-nutrients ($Si(OH)_4$, NO_3^- and

634 PO_4^{3-}), values are in $\mu mol\ L^{-1}$ $\pm 1SD$ ($n = 2$). For mean DFe concentrations, values are in $nmol\ L^{-1}$,

635 $\pm 1SD$ ($n \geq 4$).

636 **Figure 5.** Results from the mesocosm (700 L bag) experiment; **A.** Photosynthetic parameters

637 **B** Concentrations of BSi, NO_3^- and $Si(OH)_4$ and the isotope composition ($\delta^{30}Si_{BSi}$) of BSi

638 over the experimental period; **C**. Variation in $\delta^{30}Si_{BSi}$ during the experimental period, where f

639 is the fraction of dissolved silicon remaining (Si/Si_0, where Si_0 is the starting concentration of

640 $Si(OH)_4$ in the bag). Instrumental errors for $\delta^{30}Si$ values are 0.2 ‰ (2SE). A fractionation

641 factor (α) of 0.9989 was calculated using a SOLVER based algorithms to fit a model

642 (equation 4) to the data and closely resembles the reported fractionation factor (ε) of -1.2 $\pm$

643 0.02 ‰ for diatoms in the field (Fripiat et al., 2011). Also present is the model (equation 2)

644 for evolution of $\delta^{30}Si(OH)_4$ during the experiment.

645 **Figure 6.** Microscope images of *Asterionelopsis glacilis* and *Mellosira moniliformis*. *A.*

646 *glacilis* is a pennate diatom (general length, 30 – 150 µm), while *M. moniliformis* is a centric

647 diatom (Length, 11-30 µm, diameter, 17 – 70 µm).

648 **Figure 7.** Change in **A.** photosynthetic parameters B. POC, PON and BSi concentration C.

649 and elemental ratios for microcosm (20 L) experiment harvested after 96 hours incubation

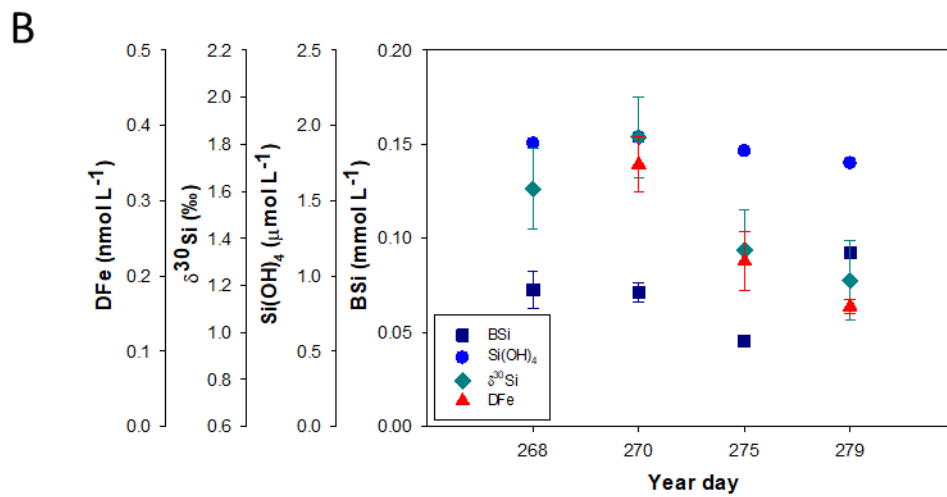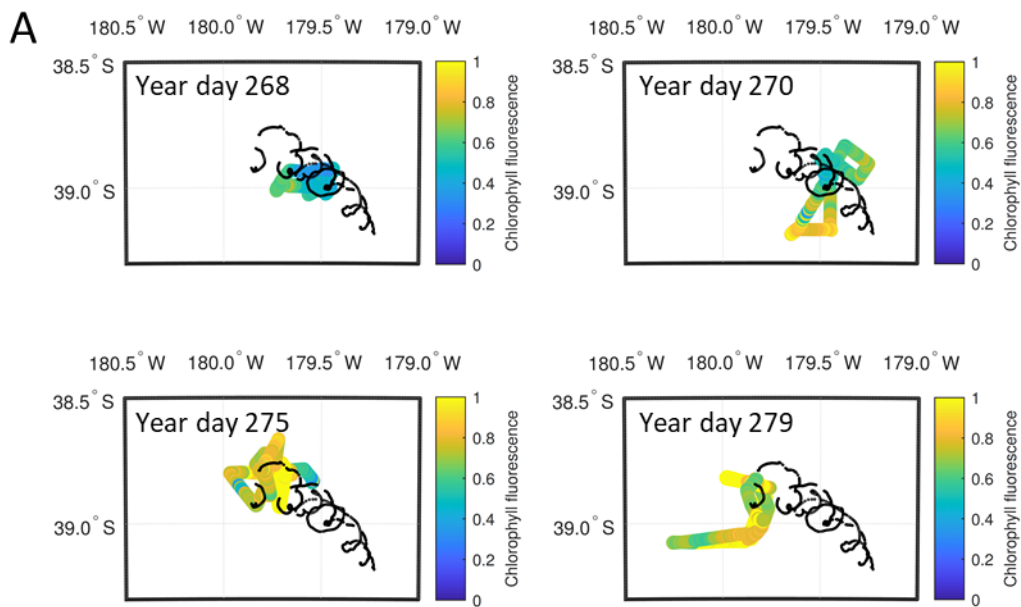650 time. Experiments represents T0, control and Fe-addition experiments.
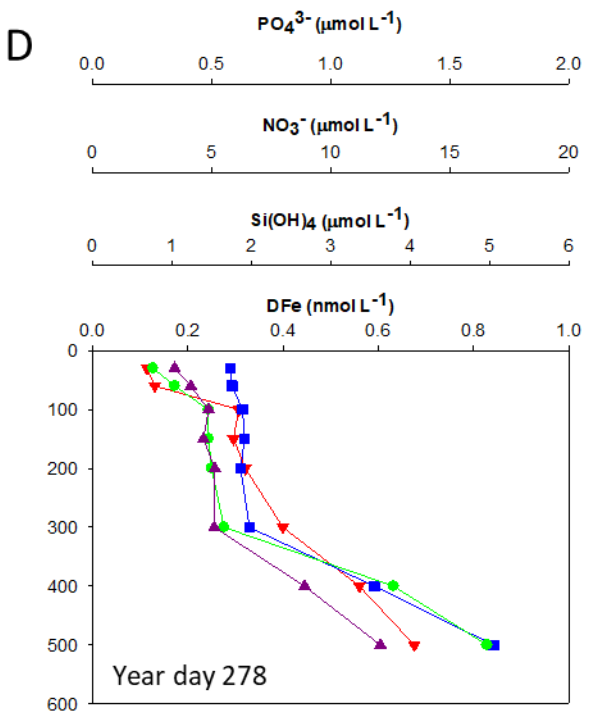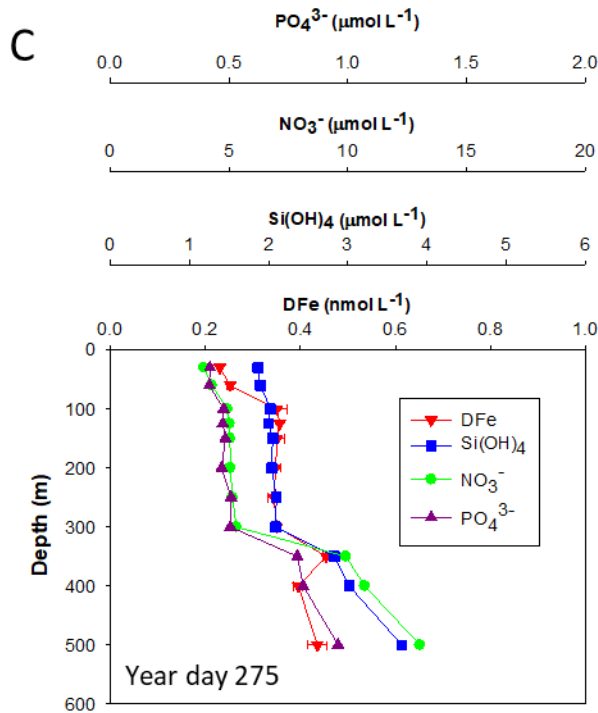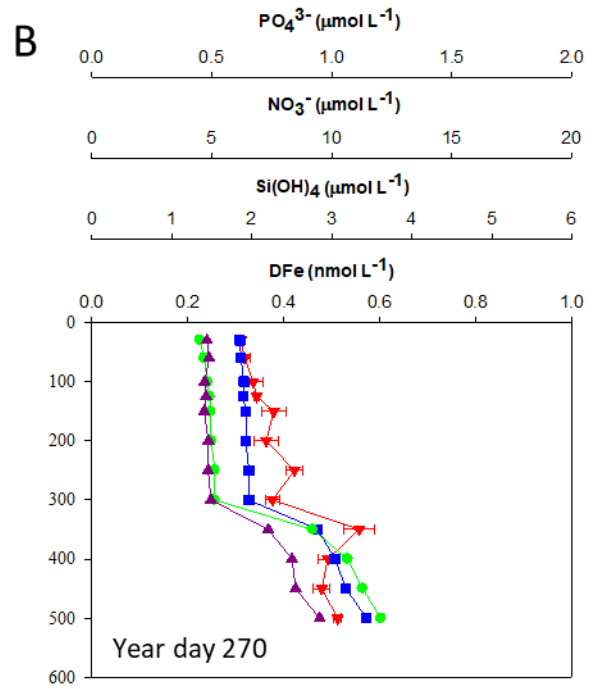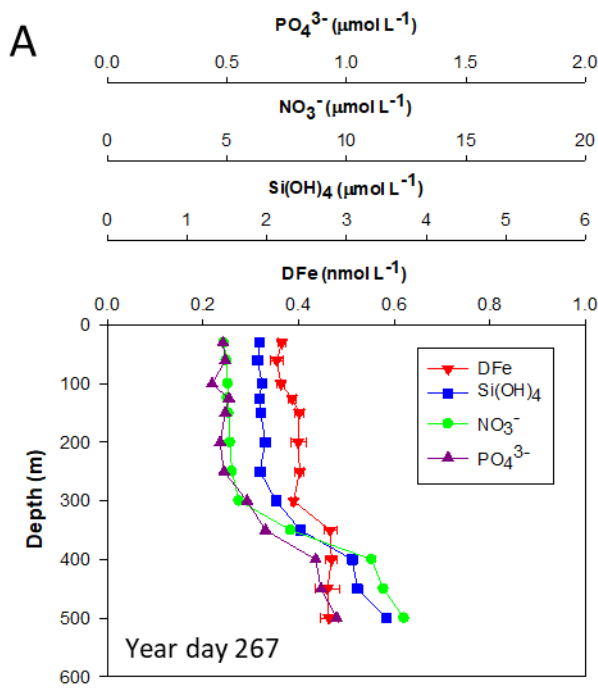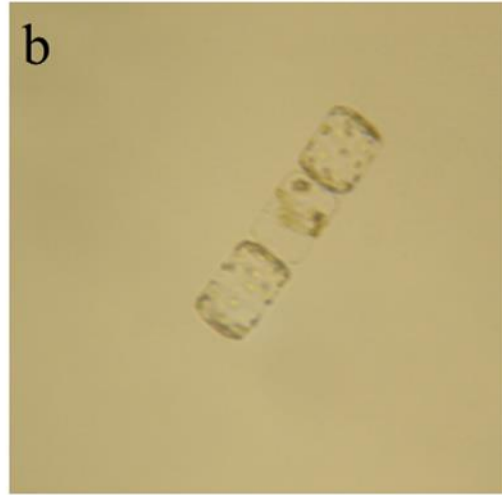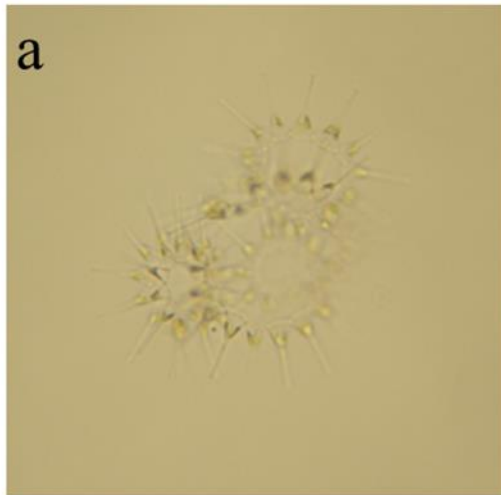
651
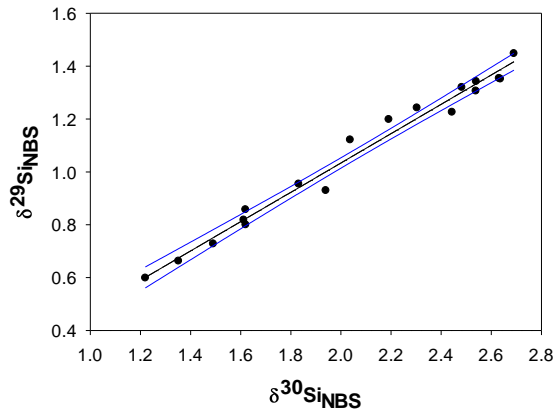
652

653

654

655

656

657

658

659

660

661

668

669